

A Method for Retrieving Land Surface Reflectance Using MODIS Data

Jie Guang, Yong Xue, *Senior Member, IEEE*, Leiku Yang, Linlu Mei, and Xingwei He

Abstract—Surface reflectance retrieval is an important step in the data processing chain for the extraction of quantitative information in many applications. The aim of this paper is to develop a method for retrieving surface reflectance and aerosol optical depth simultaneously over both dark vegetated surfaces and bright land surfaces. After applying this method to the Moderate Resolution Imaging Spectroradiometer (MODIS) data in the Heihe River Basin of China, aerosol optical depth and surface reflectance values of these regions are calculated. The retrieved surface reflectance from MODIS is consistent with measured reflectance from Analytical Spectral Device (ASD) Field Spec spectral radiometer, with R-squared (R^2) greater than 0.84 and root mean square error (RMSE) of 0.027 at band 1 (0.66 μm), 0.015 at band 3 (0.47 μm), and 0.017 at band 4 (0.55 μm). The R^2 of MOD09 with ASD measured surface reflectance is around 0.60, and RMSE are 0.049 at band 1, 0.024 at band 3, and 0.036 at band 4.

Index Terms—Surface reflectance, MODIS, BRDF, land, simultaneous.

I. INTRODUCTION

SURFACE reflectance retrieval is an important step in the data processing chain for the extraction of quantitative information in many applications. In order to obtain the real surface reflectance, atmospheric correction is absolutely a necessary processing step to deal with the space or aircraft-borne remote sensing data. However, precise atmospheric correction does not only require the directional reflectance (or radiation) characteristics of the land surface [1], but also requires the coinstantaneous parameters of atmosphere when the sensors pass by. The high spatial and temporal variability of atmospheric aerosols scattering represents the greatest uncertainty in derivation of surface reflectance over land [2]. However, decoupling

Manuscript received September 29, 2012; revised January 18, 2013 and April 08, 2013; accepted April 11, 2013. Date of publication June 05, 2013; date of current version June 17, 2013. This work was supported in part by NSFC, China under Grant 41101323, and by the Ministry of Science and Technology (MOST) of China under Grant 2013CB733403. (*Corresponding author: Y. Xue.*)

J. Guang, L. Mei, and X. He are with the Key Laboratory of Digital Earth Science, Institute of Remote Sensing and Digital Earth, Chinese Academy of Sciences, Beijing 100094, China (e-mail: guangjier@163.com; meilinlu@163.com; hexingweiph@163.com).

Y. Xue is with the Key Laboratory of Digital Earth Science, Institute of Remote Sensing and Digital Earth, Chinese Academy of Sciences, Beijing 100094, China, and also with the Faculty of Life Sciences and Computing, London Metropolitan University, London N7 8DB, U.K. (e-mail: yx9@hotmail.com).

L. Yang is with the State Key Laboratory of Remote Sensing Science, Jointly Sponsored by Beijing Normal University and Institute of Remote Sensing and Digital Earth of Chinese Academy of Sciences (CAS), Beijing Normal University, Beijing 100875, China (e-mail: leiku.yang@gmail.com).

Color versions of one or more of the figures in this paper are available online at <http://ieeexplore.ieee.org>.

Digital Object Identifier 10.1109/JSTARS.2013.2259145

the atmospheric and surface scattering contribution of the satellite signal is difficult. On the one hand, accurate knowledge of the magnitude and variations in surface reflectance is mandatory in order to retrieve aerosol properties from satellite [3]. The Moderate Resolution Imaging Spectroradiometer (MODIS) aerosol products are retrieved by two distinct algorithms: the Dark Target (DT) and the Deep Blue (DB) in NASA. Both algorithms regard surface reflectance as a prior knowledge. The MODIS DT aerosol optical depth (AOD) retrieval is based on the relationship between the surface reflectance at visible (VIS) and shortwave infrared (SWIR) [4], which provides reasonable good accuracy of AODs for most vegetated land surfaces but generally shows low accuracy of AODs for arid, semi-arid, urban, desert areas. DB algorithm determines the surface reflectance of a given pixel from a clear-scene database based upon its geolocation [5]. On the other hand, surface reflectance retrieval requires knowledge of aerosol parameters. MODIS surface reflectance product (MOD09) is inverted with the help of the Second Simulation of a Satellite Signal in the Solar Spectrum, Vector (6S) model using atmospheric inputs taken from the National Centers for Environmental Prediction (NCEP) (ozone, pressure) or directly derived the MODIS data (aerosol, water vapor). AOD is estimated by comparing actual corrected top-of-atmosphere values to modeled top-of-atmosphere values with known amounts of AOD added. The derived AOD is then used in a second pass of atmospheric correction [6], [7]. Because of this dilemma, a simultaneous inversion of surface and aerosol properties is practiced in some previous studies [8]–[12].

Based on a solution of the radiative transfer equation, Xue and Cracknell [13] proposed a formula describing the relation between the ground surface reflectance A and TOA reflectance A' . Tang *et al.* [8] applied this approach to MODIS and developed the Synergy of TERRA and AQUA MODIS data (SYNTAM) method, which has proved to be useful in AOD retrieval for various ground surfaces, including for high reflective surface [14]. Guang *et al.* [15] have developed this model for considering the surface bidirectional reflectance distribution function (BRDF) effects during AOD retrieval, which not only can estimate AOD from MODIS data but also can obtain the BRDF parameters simultaneously.

Based on a similar principle addressed by Guang *et al.* [15], this paper focus on using this model to retrieve surface reflectance from MODIS data and evaluate the precision of retrieved surface reflectance. Section II describes the model. The study area and data used in this paper are introduced in Section III. The retrieval results are analyzed and validated in Section IV. Finally, we summarize the advantages of this new model and discuss the uncertainties in Section V.

TABLE I
 ASD IN SITU MEASUREMENTS DATE, LAND COVER AND POSITIONAL
 INFORMATION

Period of Measurement	Stations	land cover	Location
June 3, 2008	Linze grassland	Saline land	39.24° N, 100.07° E
May 23, 2008	Linze station 1	Corn	39.35° N, 100.13° E
May 25, 28, 30 and June 16, 2008	Linze station 2	Corn	39.33° N, 100.14° E
May 28, 30 and June 16, 2008	Linze station 3	desert steppe	39.36° N, 100.15° E
June 16 and July 1, 2008	Huazhaizi station 1	desert steppe	38.75° N, 100.31° E
July 11, 2008	Huazhaizi station 2	desert steppe	38.77° N, 100.32° E
June 16 and July 1, 2008	Huazhaizi station 3	Corn	38.77° N, 100.35° E
May 30, June 1, 3, 4, 16, 29 and July 1, 7, 2008	Yingke oasis 1	Corn	38.85° N, 100.41° E
May 20, 30, June 1, 3, 4, 29 and July 1, 7, 2008	Yingke oasis 2	Wheat	38.87° N, 100.42° E
July 6, 2008	Biandukou station 1	Grass	38.22° N, 100.98° E
June 24, 2008	Biandukou station 2	Cole	38.20° N, 100.99° E

II. METHODOLOGIES

The relationship between TOA reflectance, AOD and surface BRDF was developed in order to retrieve both AOD and surface BRDF parameters [15]. The expression of the retrieval model is shown in (1) to (12).

Here, A_{j,λ_i} is ground surface reflectance at wavelength λ . A'_{j,λ_i} is top of atmosphere (TOA) reflectance at wavelength λ . $j = 1$ or 2 stands for the observation of Terra-MODIS and Aqua-MODIS, respectively. The central wavelengths of the visible bands are 0.66 , 0.47 and $0.55 \mu\text{m}$ for $i = 1, 2$ and 3 , respec-

tively. λ_i is the central wavelength of band i ; ε is the backscattering coefficient, typically 0.1 ; $a = \sec \theta_s$; $b = 0.21 \sec \theta_s + 1.78$; θ_s is the solar zenith angle and θ_v is the sensor zenith angle. ϕ is the view-sun relative azimuth angle.

$K_{\text{vol}}(\theta_{s,j}, \theta_{v,j}, \phi_j)$ and $K_{\text{geo}}(\theta_{s,j}, \theta_{v,j}, \phi_j)$ are BRDF model kernels, the Ross-Thick and the Li-Sparse-Reciprocal (RTLSR) kernel respectively, which are used in the operational MODIS BRDF/Albedo algorithm and tested to be well suited to describe the surface anisotropy of the variety of land covers that are distributed world-wide [16]. $f_{\text{iso}}(\lambda_i)$, $f_{\text{vol}}(\lambda_i)$ and $f_{\text{geo}}(\lambda_i)$ are the BRDF kernel model parameters, the isotropic parameter, the volumetric parameter and the geometric parameter, where

$$K_{\text{vol}}(\theta_{s,j}, \theta_{v,j}, \phi_j) = \frac{(\pi/2 - \xi) \cos \xi + \sin \xi}{\cos \theta_{s,j} + \cos \theta_{v,j}} - \frac{\pi}{4} \quad (3)$$

$$\cos \xi = \cos \theta_{s,j} \cos \theta_{v,j} + \sin \theta_{s,j} \sin \theta_{v,j} \cos \phi_j \quad (4)$$

$$K_{\text{geo}}(\theta_{s,j}, \theta_{v,j}, \phi_j) = O(\theta_{s,j}, \theta_{v,j}, \phi_j) - \sec \theta'_{s,j} - \sec \theta'_{v,j} + \frac{1}{2}(1 + \cos \xi') \sec \theta'_{s,j} \sec \theta'_{v,j} \quad (5)$$

$$O = \frac{1}{\pi}(t - \sin t \cos t)(\sec \theta'_{s,j} + \sec \theta'_{v,j}) \quad (6)$$

$$\cos t = \frac{2\sqrt{D^2 + (\tan \theta'_{s,j} \tan \theta'_{v,j} \sin \phi_j)^2}}{\sec \theta'_{s,j} + \sec \theta'_{v,j}} \quad (7)$$

$$D = \sqrt{\tan^2 \theta'_{s,j} + \tan^2 \theta'_{v,j} - 2 \tan \theta'_{s,j} \tan \theta'_{v,j} \cos \phi_j} \quad (8)$$

$$\cos \xi' = \cos \theta'_{s,j} \cos \theta'_{v,j} + \sin \theta'_{s,j} \sin \theta'_{v,j} \cos \phi_j \quad (9)$$

$$\theta'_{s,j} = \tan^{-1}(\tan \theta_{s,j}) \quad (10)$$

$$\theta'_{v,j} = \tan^{-1}(\tan \theta_{v,j}) \quad (11)$$

As the BRDF parameters (f_{iso} , f_{vol} , f_{geo}) vary with wavelength, we should derive a relationship between BRDF parameters on different wavelengths to reduce the number of unknown parameters. Based on statistical analysis of MODIS BRDF products (MCD43B1), a linear relation between the BRDF parameters of band 1 ($0.66 \mu\text{m}$) and band 3 ($0.47 \mu\text{m}$) as well as band 1 and band 4 ($0.55 \mu\text{m}$) are found:

$$f_m(\lambda_n) = a_{mn} f_m(\lambda_{0.66}) + b_{mn} \quad (12)$$

where $m = 1, 2, 3$ stands for subscripts 'iso', 'vol' and 'geo', respectively, on the BRDF parameter f ; $n = 1, 2$ stands for band 3 and band 4 of central wavelength of 0.47 , $0.55 \mu\text{m}$, respectively; a_{mn} , b_{mn} are constant, which can be derived from historical MODIS BRDF products (MCD43B1). $\lambda_{0.66}$ means $0.66 \mu\text{m}$.

With respect to the actual computation, six parameters should be solved: α , β_1 , β_2 in the Ångström turbidity formula and f_{iso}

$$A_{j,\lambda_i} = \frac{(A'_{j,\lambda_i} b_j - a_j) + a_j(1 - A'_{j,\lambda_i})e^{(a_j - b_j)\varepsilon(0.00879\lambda_i^{-4.09} + \beta_j \lambda_i^{-\alpha}) \sec \theta_{v,j}}}{(A'_{j,\lambda_i} b_j - a_j) + b_j(1 - A'_{j,\lambda_i})e^{(a_j - b_j)\varepsilon(0.00879\lambda_i^{-4.09} + \beta_j \lambda_i^{-\alpha}) \sec \theta_{v,j}}} \quad (1)$$

$$A_{j,\lambda_i} = f_{\text{iso}}(\lambda_i) + f_{\text{vol}}(\lambda_i)K_{\text{vol}}(\theta_{s,j}, \theta_{v,j}, \phi_j) + f_{\text{geo}}(\lambda_i)K_{\text{geo}}(\theta_{s,j}, \theta_{v,j}, \phi_j) \quad (2)$$

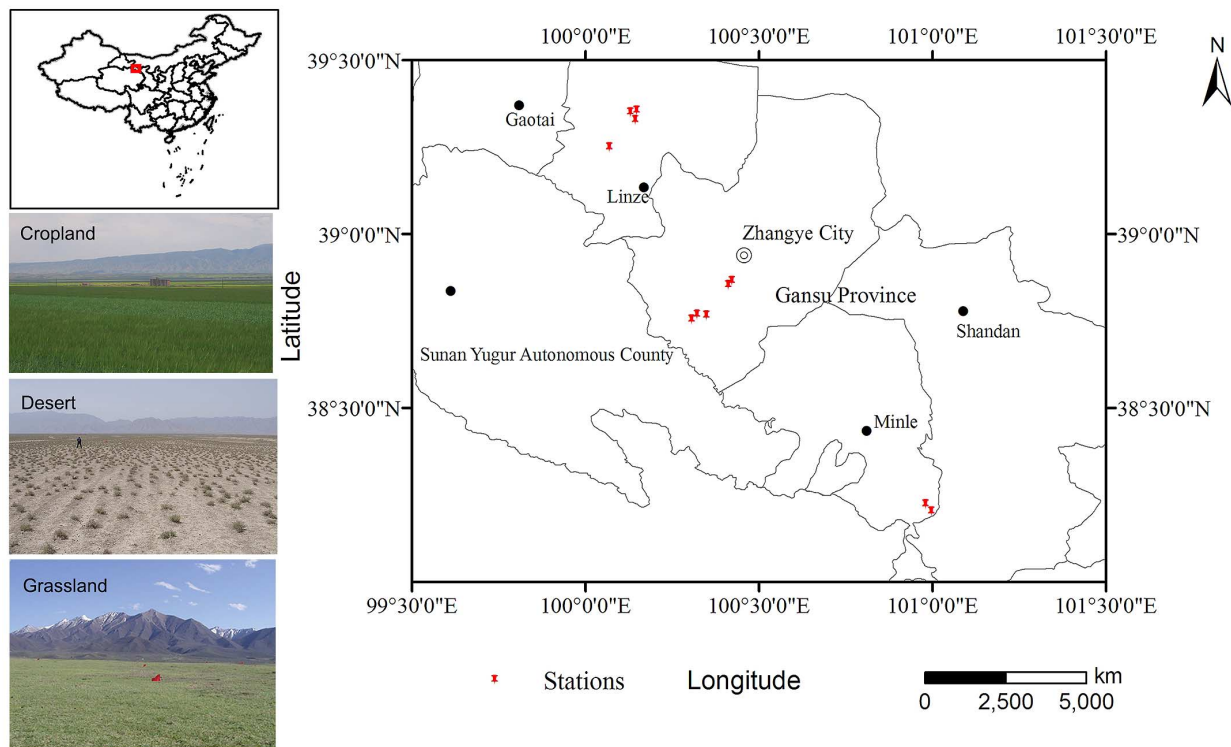


Fig. 1. Geographical locations of the stations and some real photos of the stations.

$(\lambda_{0.66})$, $f_{vol}(\lambda_{0.66})$, $f_{geo}(\lambda_{0.66})$ in the kernel-driven BRDF model. Substituting Terra and Aqua MODIS three visible bands (0.47, 0.55, 0.66 μm) data for the above non-linear equations, a closed non-linear system of equations is obtained. Because of the difficulty in obtaining the analytical solution of nonlinear equations, a Newton iteration algorithm is used to get the numerical solutions in this paper. The globally-convergent Newton numerical method was used to solve a system of n non-linear equations in n dimensions. The keywords of Newton method are set as follows: the maximum allowed number of iterations is 10000. The scaled maximum step length allowed in line search is 0.005. The convergence criterion on the function values is set to 0.005. The convergence criterion on X is set to 0.001 [17].

III. DATA ACQUISITION AND PREPROCESSING

The research area is in the Heihe River Basin (97°–103°E, 36°–42°N) which lies in the arid region of northwest China. Geographic differentiation in the basin is evident. From the south to the north of the basin, there are three major geomorphological units: the southern Qilian Mountains, the middle Hexi Corridor and the northern Alxa High-plain. Most measurements were made in the middle Hexi Corridor—an area of desert, sandy desert, bare Gobi, irrigated farmland, meadow, marsh and residential area.

The Watershed Allied Telemetry Experimental Research (WATER) is a simultaneous airborne, satellite-borne, and ground-based remote sensing experiment taking place in the Heihe River Basin in 2008 [18]. Ground measurements for our validation purposes mainly include surface reflectance

spectra of a variety of cover types measured with an Analytical Spectral Device (ASD) Field Spec spectral radiometer (covering the spectrum of 0.35–2.5 μm). A series of field campaigns were carried out from March to July 2008 to measure surface reflectance by the ASD spectral radiometers. The in situ ASD measurements date, land cover and positional information are shown in Table I and Fig. 1. It is important to measure surface reflectance spectra simultaneously with the satellite overpass over homogeneous plots of different cover types. Desert distributed between Zangye Oasis and the Qilian Mountains, relatively homogeneous covered with dwarf shrub vegetation dominated by *Haloxylon ammodendron* (C.A.Mey.) Bge. Under the influence of occasional streams flowing from the Qilian Mountains, there are low ditches but a very small percentage among the desert. We measured the mixed spectra of crop and soil in the row-planted corn field in Yingke Oasis to represent the mean reflectance of that field (plot). Grassland in the Biandukou of Minle County is very homogeneous, while the cole fields there are mixed by cole flowers and soils. In a typical field campaign for surface reflectance measurements, we usually carried the ASD spectral radiometer measured surface reflectance over three or four homogenous fields (plots) during the period of the satellite overpass ($\pm 1\text{h}$). In each field, 50–100 points along several transects were measured. A white reference panel was measured every point or every few points, depending on the atmospheric conditions. The average reflectance of these points was used to represent the mean reflectance of that field (plot).

The remote sensing data used in this study consist of MODIS L1B data of Terra and Aqua (MOD02 and MYD02), MODIS

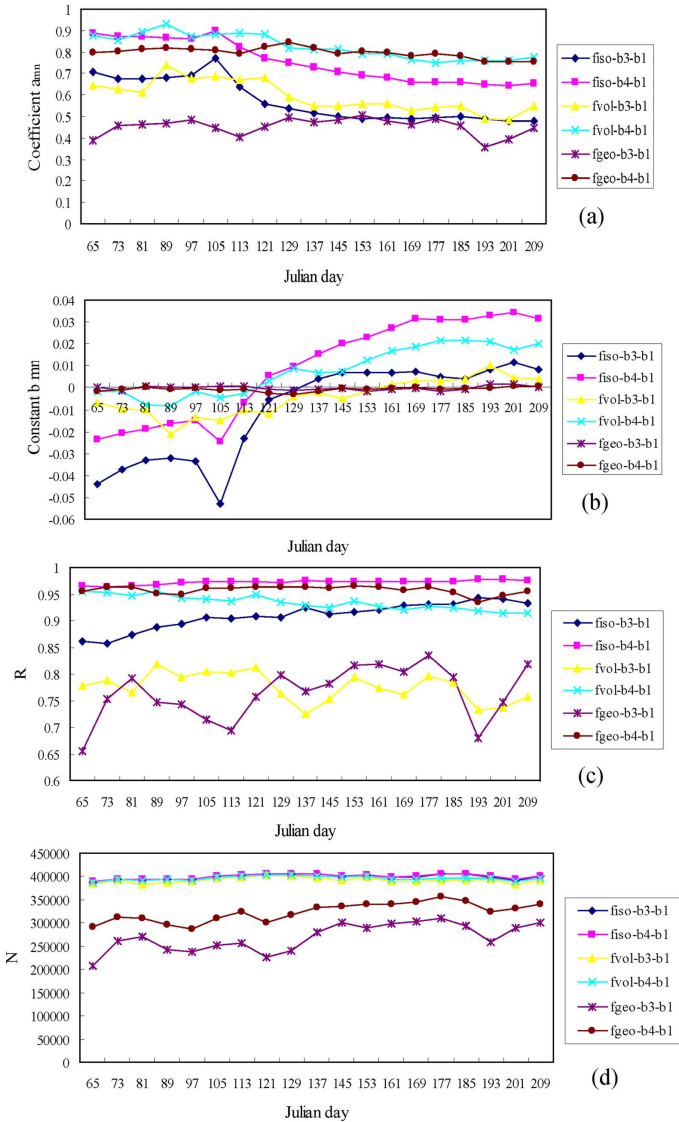


Fig. 2. The relationship between kernel parameters f_{iso} , f_{vol} and f_{geo} of different bands in the Heihe River Basin in March to July 2008: (a) the coefficient a_{mn} , (b) the constant b_{mn} , (c) correlation coefficients (R) and (d) sampling numbers (N). f_{iso} -b3-b1 stands for “the linear relationship between f_{iso} of band 1 and band 3”. The rest may be deduced by analogy.

BRDF/Albedo product (MCD43B1) and MODIS Level 2 aerosol product (MOD04/MYD04). As MODIS L1B data are already calibrated, the preprocessing of MODIS data mainly includes image geometric correction, two temporal image registrations, and image subsetting. The size of these images is 700×600 pixels with spatial resolution at 1 km after preprocessing. As we focus on discussing the feasibility of our model, the detailed algorithm of pre-processing of data is not described in this paper. The BRDF model kernel weights f_{iso} , f_{vol} , and f_{geo} depend on spectral bands and vary with time and location. They are provided by the MCD43B1 product data at 1 km resolution over the globe for every 16-day composite period [19]. Collection 005 changed the phased production strategy and produced every 8 days with 16 days of acquisition. Using MRT (MODIS Reprojection Tool), MCD43B1 product data are geolocated, reprojected and resized. Cloud detection and mask are following the same method in [20].

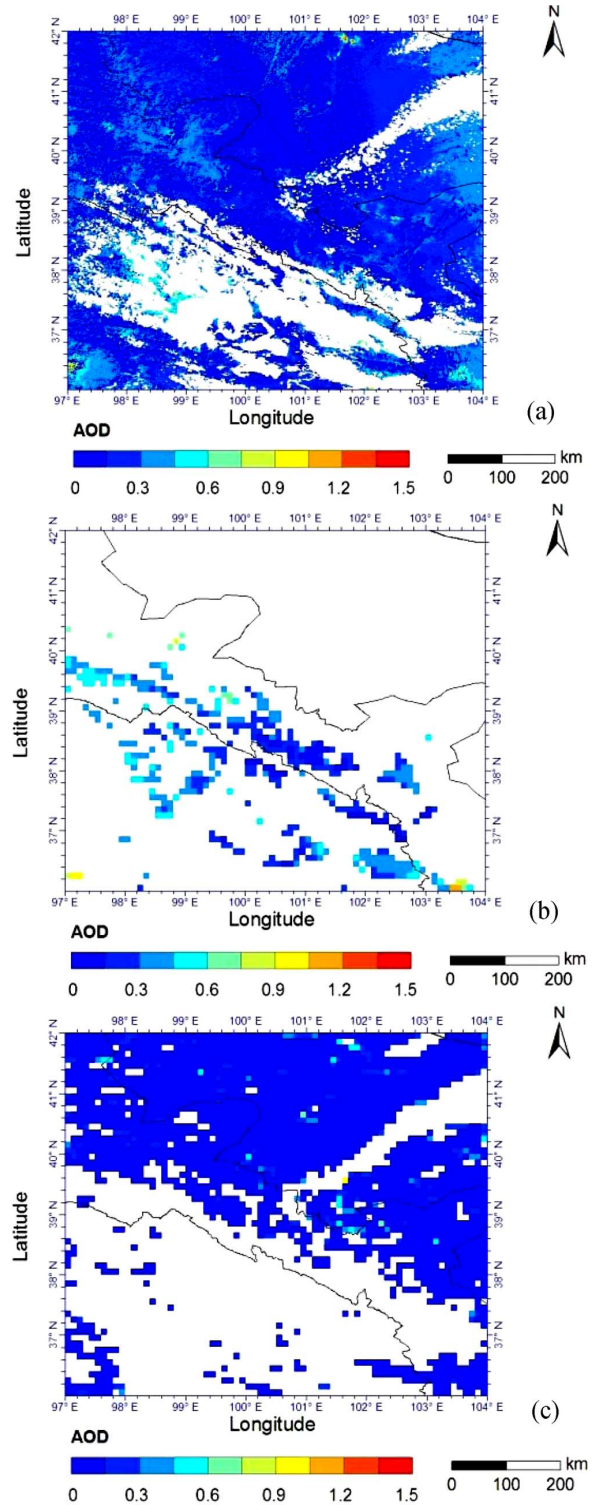


Fig. 3. (a) Retrieved AOD, (b) MODIS aerosol product (MYD04) of Dark Target, (c) MODIS aerosol product (MYD04) of Deep Blue in band 4 on June 16, 2008 of Aqua/MODIS. White pixels indicate the clouds or gaps due to inversion failure.

IV. RESULTS AND DISCUSSION

The linear relationship between band 1 and band 3 as well as band 1 and band 4 of the MODIS BRDF/Albedo product (MCD43B1) in the Heihe River Basin of China in March to July 2008 are shown in Fig. 2.

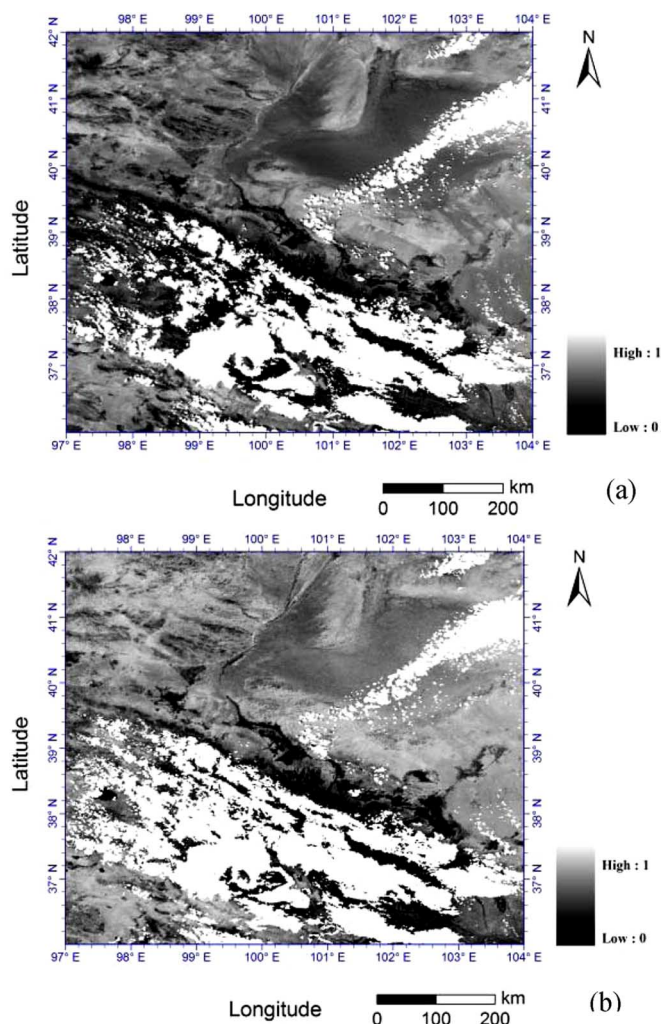


Fig. 4. (a) Top-of-atmosphere reflectance, (b) retrieved surface reflectance in band 4 on June 16, 2008 of Aqua/MODIS. White pixels indicate the clouds or gaps due to inversion failure.

The correlation coefficient between kernel-driven parameters of bands 1 and 4 is greater than 0.91, and greater than 0.65 of bands 1 and 3. This suggests that linear models can be accepted as good approximations to describe the relation between kernel-driven parameters of different bands, at least over a limited area. The kernel-driven parameters f_{iso} and f_{vol} have a big change in winter and a small change in summer, which are concerned with Leaf Area Index (LAI) and the surface reflectance, while the kernel-driven parameter f_{geo} is relatively stable at a fixed pixel as the geometric parameter is a function of crown/object density and size, only related to surface roughness (gapiness of the landscape) [21].

This study implements the model using Terra and Aqua MODIS L1B data to derive AOD, the kernel-driven parameters and surface reflectance in the days when in situ ground measurements were carried out. AOD retrieval result was compared to NASA MODIS aerosol products (Dark Target and Deep Blue algorithm) on June 16, 2008 and shown in Fig. 3. Although MODIS AOD products are in very good quality, the MODIS products of Dark Target (DT) version and Deep Blue (DB) version are not consistent. As shown in Fig. 3, there

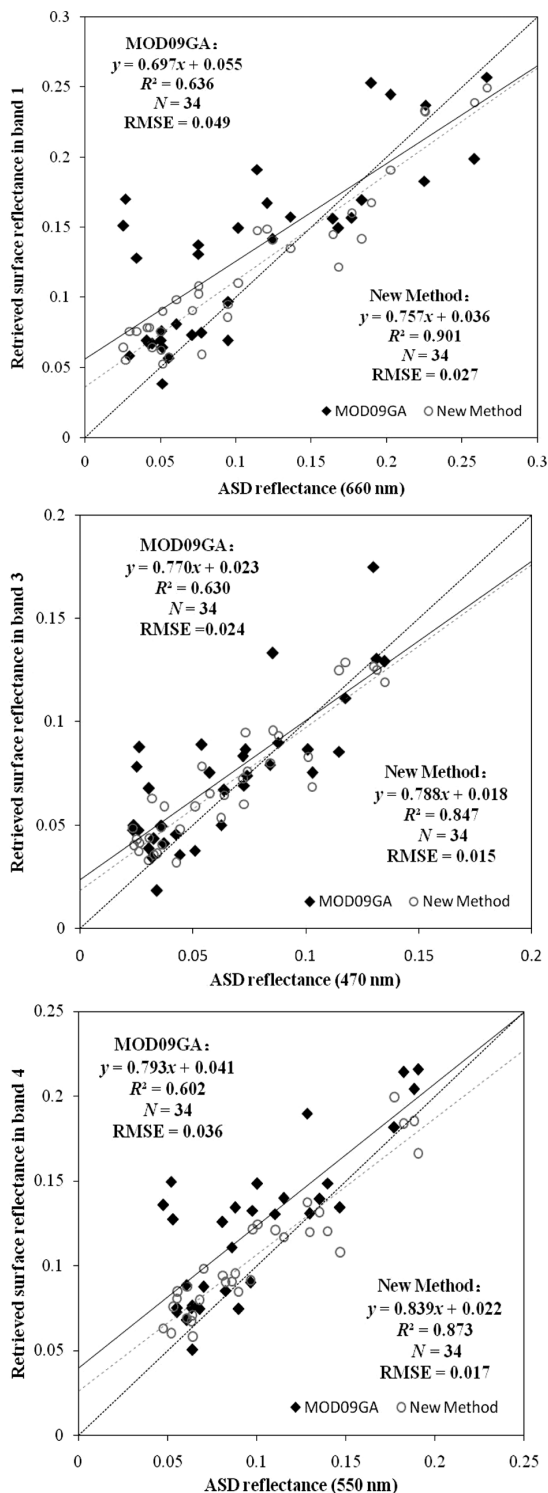


Fig. 5. Retrieved surface reflectance from this method and from MOD09 surface reflectance products plotted as functions of ground observations with ASD Field Spec spectral radiometer measurements of band 1, band 3 and band 4. Diamond and solid line shows the data from MOD09 products. Circle and dash line shows the result from this method.

are many gaps in the MODIS AOD aerosol product which indicates that the DT algorithm used for obtaining MODIS AOD products should be improved in high-reflectivity surfaces. However, our model can retrieve AOD over both vegetated and

non-vegetated (bright) surfaces. Fig. 4 shows the top-of-atmosphere reflectance as well as surface reflectance retrieved from Aqua/MODIS on June 16, 2008.

To validate the retrieved surface reflectance, in situ ASD measurements were conducted in the way described in Section III. Retrieved surface reflectance from this method and from MODIS surface reflectance products (MOD09) plotted as functions of ground observations are shown in Fig. 5. The retrieved surface reflectance from MODIS is consistent with measured reflectance from ASD Field Spec spectral radiometer, with R-squared (R^2) greater than 0.84 and root mean square error (RMSE) of 0.027 at band 1 (0.66 μm), 0.015 at band 3 (0.47 μm), and 0.017 at band 4 (0.55 μm). The R^2 of MOD09 with ASD measured surface reflectance is around 0.60, and RMSE are 0.049 at band 1, 0.024 at band 3, and 0.036 at band 4. One of the possible error sources of the MOD09 product is the inaccurate atmospheric input parameter in this study area, mainly aerosol optical depth and water vapor content.

V. CONCLUSION

This paper introduced an approach to retrieve surface reflectance from MODIS data. This approach considers the surface BRDF effects during retrieval and can estimate surface reflectance and AOD simultaneously. Besides, this method both suitable for vegetated surfaces and bright land surfaces. This is quite important for the atmospheric correction research. Using ASD measurements to validate retrieved surface reflectance, the RMSE is lower than 0.03 and R^2 values are greater than 0.84.

The possible sources of errors in this method include performance degradation of MODIS onboard two satellites, two temporal images matching, sub-pixel cloud contamination, which should be taken into account in future research. The statistical relationship between kernel-driven model parameters used in this paper may not tenable in other areas. More extensive experiments and validations are still needed under different conditions for a global implementation.

ACKNOWLEDGMENT

The authors would like to thank the reviewers and the editors for their constructive and helpful suggestions.

The surface reflectance measured using ASD in the Heihe River Basin are from experiments (<http://rsdc.bnu.edu.cn>) supported by the Chinese State Key Basic Research Project under Grant 2007CB714407 and by the auspices of CAS Action Plan for West Development Programme (Grant KZCX2-XB2-09).

REFERENCES

- [1] Y. Wang, A. I. Lyapustin, J. L. Privette, R. B. Cook, S. K. Santhana-Vannan, E. F. Vermote, and C. L. Schaaf, "Assessment of biases in MODIS surface reflectance due to Lambertian approximation," *Remote Sens. Environ.*, vol. 114, pp. 2791–2801, 2010.
- [2] S. Y. Kotchenova, E. F. Vermote, R. Levy, and A. Lyapustin, "Radiative transfer codes for atmospheric correction and aerosol retrieval: Intercomparison study," *Appl. Optics*, vol. 47, pp. 2215–2226, 2008.
- [3] O. Dubovik and M. D. King, "A flexible inversion algorithm for retrieval of aerosol optical properties from sun and sky radiance measurements," *J. Geophys. Res.*, vol. 105, pp. 20673–20696, 2000.
- [4] R. C. Levy, L. A. Remer, S. Mattoo, E. Vermote, and Y. J. Kaufman, "Second generation algorithm for retrieving aerosol properties over land from MODIS spectral reflectance," *J. Geophys. Res.*, vol. 112, no. D13211, pp. 1–21, 2007.
- [5] N. C. Hsu, S.-C. Tsay, M. King, and J. R. Herman, "Deep blue retrievals of Asian aerosol properties during ACE-Asia," *IEEE Trans. Geosci. Remote Sens.*, vol. 44, pp. 3180–3195, 2006.
- [6] E. F. Vermote, N. Z. E. Saleous, and C. O. Justice, "Atmospheric correction of the MODIS data in the visible to middle infrared: First results," *Remote Sens. Environ.*, vol. 83, no. 1–2, pp. 97–111, 2002.
- [7] E. F. Vermote, S. Y. Kotchenova, and J. P. Ray, "MODIS surface reflectance user's guide, version 1.3," MODIS Land Surface Reflectance Science Computing Facility, 2011 [Online]. Available: <http://modis-sr.ldr.org>
- [8] J. Tang, Y. Xue, T. Yu, and Y. Guan, "Aerosol optical depth determination by exploiting the synergy of Terra and Aqua MODIS," *Remote Sens. Environ.*, vol. 94, pp. 327–334, 2005.
- [9] W. von Hoyningen Huene, A. A. Kokhanovsky, J. P. Burrows, V. Bruniquel-Pinel, P. Regner, and F. Baret, "Simultaneous determination of aerosol and surface characteristics from MERIS top-of-atmosphere reflectance," *Advan. Space Res.*, vol. 37, pp. 2172–2177, 2006.
- [10] J. Keller, S. Bojinski, and A. S. H. Prevot, "Simultaneous retrieval of aerosol and surface optical properties using data of the multi-angle imaging spectroradiometer (MISR)," *Remote Sens. Environ.*, vol. 107, pp. 120–137, 2007.
- [11] D. Carrer, J. L. Roujean, O. Hautecoeur, and T. Elias, "Daily estimates of aerosol optical thickness over land surface based on a directional and temporal analysis of SEVIRI MSG visible observations," *J. Geophys. Res.*, vol. 115, no. D10208, pp. 1–24, 2010.
- [12] J. Guang, Y. Xue, Y. Wang, Y. Li, L. Mei, H. Xu, S. Liang, J. Wang, and L. Bai, "Simultaneous determination of aerosol optical thickness and surface reflectance using ASTER visible to near-infrared data over land," *Int. J. Remote Sens.*, vol. 32, pp. 6961–6974, 2011.
- [13] Y. Xue and A. P. Cracknell, "Operational bi-angle approach to retrieve the Earth surface albedo from AVHRR data in the visible band," *Int. J. Remote Sens.*, vol. 16, pp. 417–429, 1995.
- [14] L. Mei, Y. Xue, H. Xu, J. Guang, Y. J. Li, Y. Wang, J. W. Ai, S. Z. Jiang, and X. W. He, "Validation and analysis of aerosol optical thickness retrieval over land," *Int. J. Remote Sens.*, vol. 33, no. 3, pp. 781–803, 2012.
- [15] J. Guang, Y. Xue, Y. Li, S. Liang, L. Mei, and H. Xu, "Retrieval of aerosol optical depth over bright land surfaces by coupling bidirectional reflectance distribution function model and aerosol retrieval model," *Remote Sens. Lett.*, vol. 3, no. 409, pp. 577–584, 2012.
- [16] C. B. Schaaf, J. Liu, F. Gao, and A. H. Strahler, B. Ramachandran, C. Justice, and M. Abrams, Eds., "MODIS albedo and reflectance anisotropy products from Aqua and Terra," in *Land Remote Sensing and Global Environmental Change: NASA's Earth Observing System and the Science of ASTER and MODIS*. Berlin, Germany: Springer-Verlag, 2011, vol. 11, p. 873.
- [17] W. H. Press, S. A. Teukolsky, W. T. Vetterling, and B. P. Flannery, *Numerical Recipes: The Art of Scientific Computing*, 3rd ed. Cambridge, U.K.: Cambridge University Press, 2007.
- [18] X. Li, X. W. Li, Z. Y. Li, M. G. Ma, J. Wang, Q. Xiao, Q. Liu, T. Che, E. X. Chen, G. J. Yan, Z. Y. Hu, L. X. Zhang, R. Z. Chu, P. X. Su, Q. H. Liu, S. M. Liu, J. D. Wang, Z. Niu, Y. Chen, R. Jin, W. Z. Wang, Y. H. Ran, X. Z. Xin, and H. Z. Ren, "Watershed allied telemetry experimental research," *J. Geophys. Res.*, vol. 114, no. D22103, pp. 1–19, 2009.
- [19] C. Schaaf, F. Gao, A. Strahler, W. Lucht, X. Li, T. Tsung, N. Strugnell, X. Zhang, Y. Jin, J.-P. Muller, P. Lewis, M. Barnsley, P. Hobson, M. Disney, G. Roberts, M. Dunderdale, C. Doll, R. D'Entremont, B. Hu, S. Liang, J. Previtte, and D. Roy, "First operational BRDF, albedo and nadir reflectance products from MODIS," *Remote Sens. Environ.*, vol. 83, pp. 135–148, 2002.
- [20] L. A. Remer, Y. J. Kaufman, D. Tanré, S. Mattoo, D. A. Chu, J. V. Martins, R.-R. Li, C. Ichoku, R. C. Levy, R. G. Kleidman, T. F. Eck, E. Vermote, and B. N. Holben, "The MODIS aerosol algorithm, products, and validation," *J. Atmos. Sci.*, vol. 62, pp. 947–973, 2005.
- [21] A. H. Strahler, W. Lucht, C. B. Schaaf, T. Tsang, F. Gao, X. W. Li, J. P. Muller, P. Lewis, and M. J. Barnsley, "MODIS BRDF/albedo product: Algorithm theoretical basis document, version 5.0," 1999, NASA EOS-MODIS Doc..



Jie Guang received the M.S. degree in geographic information systems (GIS) from Nanjing Normal University, Nanjing, China, in 2006 and the Ph.D. degree in quantitative remote sensing from the Institute of Remote Sensing Applications, Chinese Academy of Sciences (CAS), Beijing, China, in 2009.

She is currently an Associate Professor at the Institute of Remote Sensing and Digital Earth (RADI), CAS. Her research interests include aerosol optical depth retrieval, land surface parameter retrieval, and BRDF modeling.



Linlu Mei received the B.S. degree in GIS from China University of Geosciences, Beijing, China, in 2008. He is currently pursuing the Ph.D. degree in quantitative remote sensing at RADI, Chinese Academy of Science (CAS), Beijing, China.

His research interests include quantitative remote sensing, aerosol science, and signal processing.



Yong Xue received the B.S. degrees in physics and the M.S. degree in remote sensing and GIS from Peking University, Beijing, China, in 1986 and 1989, respectively. He received the Ph.D. degree in remote sensing and GIS from University of Dundee, Dundee, U.K.

Dr. Xue's main research interests include aerosol optical depth retrieval, geocomputation and thermal inertia modeling. Dr. Xue is an editor of the *International Journal of Remote Sensing*, an editor of the *International Journal of Digital Earth*, a Chartered

Physicist and a member of the Institute of Physics, U.K.



Xingwei He received the B.S. degree in engineering of surveying and mapping from Xi'an University of Science and Technology, Xi'an, China, in 2009. She is currently pursuing the M.S. degree in quantitative remote sensing at RADI, Chinese Academy of Science (CAS), Beijing, China. Her research interests include remote-sensing image processing and aerosol optical depth retrieval.



Leiku Yang received the M.S. degree in photogrammetry and remote sensing from the China University of Mining and Technology, Beijing, China, in 2005. He is currently pursuing the Ph.D. degree in quantitative remote sensing at School of Geography, Beijing Normal University, China.

His research interests include BRDF modeling, satellite aerosol retrieval and atmospheric radiative transfer.